Journal of Muscle Research and Cell Motility **22**: 217–227, 2001.

Three-dimensional study of the capillary supply of skeletal muscle fibres using confocal microscopy

LUCIE KUBÍNOVÁ[1,*], JIŘÍ JANÁČEK[1], SAMO RIBARIČ[2], VITA ČEBAŠEK[3] and IDA ERŽEN[3]
[1]*Institute of Physiology, Academy of Sciences of the Czech Republic, Vídeňská 1083, 14220, Prague 4, Czech Republic;* [2]*Institute of Pathophysiology, Medical Faculty, University of Ljubljana, Zaloška 4;* [3]*Institute of Anatomy, Medical Faculty, University of Ljubljana, Korytkova 2, SI-1000, Ljubljana, Slovenia*

Received 8 March 2000; accepted in revised form 1 February 2001

Abstract

Three-dimensional (3D) study of capillary network of individual muscle fibres in rat *extensor digitorum longus* (EDL) and *soleus* (SOL) muscles is presented. Stereology and 3D reconstruction techniques were applied to stacks of serial optical sections recorded by a confocal microscope from thick muscle slices. The results suggest that SOL muscle fibres have a larger surface area and volume as well as a larger length of capillaries per fibre length than EDL. On the other hand, these two muscles have a similar ratio of capillary length to fibre surface area. The 3D approach to evaluation of muscle fibre capillarization brings many advantages over traditional measurements made on single muscle sections and could also be applied to the study of angiogenesis in other tissues.

Introduction

The capillary network (Hudlicka, 1991) provides muscle tissue with nutrition, oxygenation and removal of metabolic waste products. It adapts to changes in normal tissue, such as increased workload (Mai *et al*., 1970; Ingjer, 1979; Green *et al*., 1999) or reinnervation (Large and Tyler, 1985) and to pathological changes like hypertension (Hernandez *et al*., 1996; Koyama *et al*., 1997; Endre *et al*., 1998), kidney failure (Amann *et al*., 1998) and diabetes (Nyholm *et al*., 1997; Takeshita *et al*., 1997). Tissue survival is critically dependent on the development and remodeling of capillary network and much work has been done to understand the mechanisms controlling formation of new blood vessels (Hudlicka, 1991; Folkman and D'Amore, 1996). Recently, the potential of gene therapy to increase muscle blood supply has been evaluated in human (Isner *et al*., 1998; Murakami *et al*., 1999; Symes *et al*., 1999).

The morphometric characteristics of capillary network are usually measured in two dimensions (2D) from transverse or longitudinal tissue sections (Romanul, 1965; Mai *et al*., 1970; Brodal *et al*., 1977; Gray and Renkin, 1978; Ingjer, 1979; Large and Tyler, 1985; Egginton *et al*., 1987; Egginton and Ross, 1989a, b; Stål *et al*., 1996). The traditional, morphometrical parameter for analysing a capillary network is capillary density and is defined by the number of capillary profiles in histological sections per unit cross-sectional area (Anversa *et al*., 1989; Hudlicka *et al*., 1992) or per number of muscle fibres.

Capillaries form a network in three dimensions (3D). Therefore, from a functional point of view, the length of capillaries within a muscle sample should give a better description of a capillary network than capillary density. It is also more appropriate to directly estimate capillary length or length density. A number of stereological methods was used for measurements of capillary length or length density (for overview see Hudlicka *et al*., 1992), beginning with the model-based methods (James, 1981; Mathieu *et al*., 1983), using transverse as well as longitudinal muscle sections and providing also characteristics of capillary orientation and tortuosity. Later on, the design-based methods applied to thin sections cut in an isotropic uniform random (IUR) direction were developed (ortrip method by Mattfeldt *et al*., 1985, orientator method by Mattfeldt *et al*., 1990, isector method by Nyengaard and Gundersen, 1992) as well as the design-based methods using thick vertical slices (Gokhale, 1990, for application to capillaries see McMillan *et al*., 1994; Artacho-Perula and Roldan-Villalobos, 1995; Batra *et al*., 1995). Recently, a new approach in design-based stereology using thick slices cut in arbitrary (fixed) direction and properly software-randomized virtual probes has emerged (Kubínová and Janáček, 1998; Larsen *et al*., 1998).

The method using isotropic virtual test planes (Larsen *et al*., 1998) is especially useful in muscle capillary length measurements as transverse muscle sections (perpendicular to the muscle axis) can be used. This method is also useful for estimating capillary length/fibre length ratio in muscles providing an alternative to the classical

*To whom correspondence should be addressed: Tel.: +4202-475-2314; Fax: +4202-475-2488; E-mail: kubinova@biomed.cas.cz

capillary/fibre ratio, given by the number of capillary profiles to the number of fibre profiles in muscle cross-sections (Mall *et al*., 1987). Similarly, the capillary surface area/fibre surface area ratio is an alternative parameter to capillary/fibre perimeter ratio, when describing muscle capillarity in 3D (Mathieu-Costello, 1994).

The 3D approach to capillary network evaluation provides information on topology and course of the capillary network (i.e. number of connections between capillaries, tortuosity of capillaries). The microvascular architecture of skeletal muscles has already been studied by using vascular casting methods (Potter and Groom, 1983; Mathieu-Costello *et al*., 1988; Williams and Segal, 1992), and whole mount muscles treated with lectins. However, these methods are more appropriate for qualitative than for quantitative analysis of capillary network in 3D.

A quantitative method for evaluating muscle capillary network in 3D would thus provide new information on capillary network structure and could also be useful for testing new treatments and studying diseases that affect muscle blood supply (Nyholm *et al*., 1997; Takeshita *et al*., 1997; Isner *et al*., 1998; Murakami *et al*., 1999; Symes *et al*., 1999).

Confocal microscopy enables to obtain perfectly registered stacks of serial optical sections from thick specimens. Images of such stacks represent suitable data for quantitative measurements as well as for 3D reconstructions. Thus, new stereological methods based on evaluation of thick tissue slices cut in an arbitrary direction, using properly software-randomized virtual probes, can be easily applied and computer-based reconstructions can be made without the tedious registration of images of successive sections.

In the present study we combined 3D reconstruction techniques and stereological methods to get a new and more complex insight into the relationships between the structure of capillary network and muscle fibre types. We demonstrated how to visualize fibres and capillaries, and how to estimate different geometrical characteristics of capillaries in relation to their corresponding individual muscle fibres, e.g. the capillary length/adjacent fibre surface area or the capillary length/adjacent fibre length. The methods used are described in full detail, being relatively new and not having been used in studies of muscle capillarization yet.

3D reconstruction of the capillary network was done on two functionally different types of skeletal muscle: *extensor digitorum longus* (EDL) and *soleus* (SOL). The density of capillary network in these skeletal muscles is different and depends on the level of their oxidative metabolism, as defined by histochemical studies (Romanul, 1965; Gray and Renkin, 1978). SOL is an exclusive slow oxidative muscle with long contraction times and a higher capillary density than EDL, a fast-contracting skeletal muscle with predominance of fast glycolytic fibres, some oxidative and oxidative glycolytic fibres (Romanul, 1965; Gray and Renkin, 1978; Egginton, 1987; Eken and Gundersen, 1988, Egginton, 1990; Punkt *et al*., 1996). We assumed that the previously observed differences in capillary bed of these muscles should be clearly visualized on 3D images.

Material and methods

Animal experiments were approved by the Veterinary Administration of the Ministry for Agriculture, Forestry and Food of Slovenia, Permit 326-07-285/99. Five adult, male, Wistar rats (220–260 g body weight) were bled to death under deep ether anesthesia, and the whole EDL and SOL muscles were excised from one hind limb and frozen in liquid nitrogen. Whole cross-sections of the EDL and SOL muscle were taken in the middle of the muscle belly. The muscle sample was fixed in 2% paraformaldehyde with addition of sodiumperiodate, L-lysine and sucrose diluted in phosphate buffered saline at pH 7.2 to 7.4. After rinsing in phosphate buffered saline, muscle samples were cut into slices (less than 1 mm thick).

Immunofluorescent staining of capillaries

Tissue samples were pretreated with 5% normal swine serum (Dako, Denmark) to reduce background staining. Further they were incubated with rabbit anti-mouse IgG, raised against fibronectin (1:1300, Dako, Denmark) followed by immersion in FITC conjugated swine anti-rabbit IgG (1:20, Dako, Denmark, for details see Eržen and Maravić, 1993) and mounted in SlowFade Antifade. All antibodies were diluted in phosphate buffered saline. Serial optical sections (1 μm apart) inside a thick transverse slice of muscle were captured by a Bio-Rad MRC600 confocal laser scanning microscope (Bio-Rad Microscience Ltd., UK) using an oil immersion objective (40×, N.A. = 1.3). Then the stacks of digitized images (each of 768×512 pixels, i.e. 316×211 μm^2) were analyzed with stereological methods.

Stereological measurements

Stacks of 40 optical serial sections were sampled by a systematic uniform random sampling (Figure 1). On average five stacks (fields) were sampled per muscle specimen (Figure 2). The captured stacks were used for estimating geometrical characteristics of capillaries and fibres by new unbiased stereological methods using thick slices cut in an arbitrary direction (which was chosen as transverse in our case) and software-randomized virtual probes (Figures 3, 4). The methods were implemented exploiting our FAKIR, SLICER and SANDAU programmes to measure the capillary length/adjacent fibre surface area, capillary length/adjacent fibre length, capillary length/adjacent fibre volume, and number of capillary branchings/capillary length. More details are described below:

Firstly, fibres were sampled for the measurement by using an unbiased sampling frame (Gundersen, 1977)

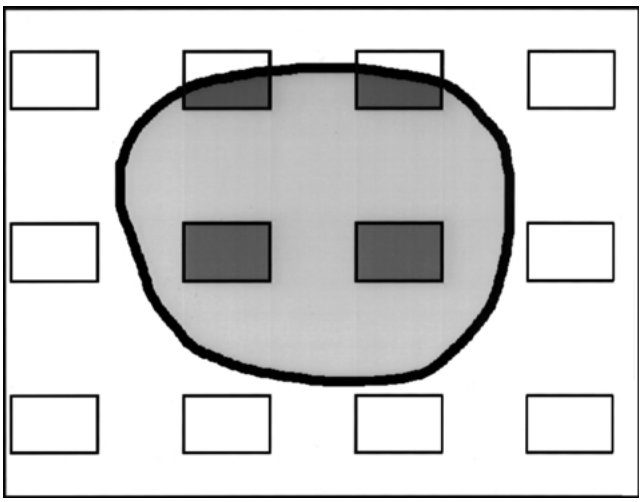

Fig. 1. Systematic uniform random sampling of random stacks of optical sections from a transverse muscle slice. The interval between stacks was chosen to be 1 mm in both x and y direction. Within those intervals a random position of the system of fields of view (frames with black outlines) was sampled. The fields intersecting the muscle section (light gray) were sampled for the measurement, i.e. stacks of images from these fields (dark gray) were recorded by a confocal microscope.

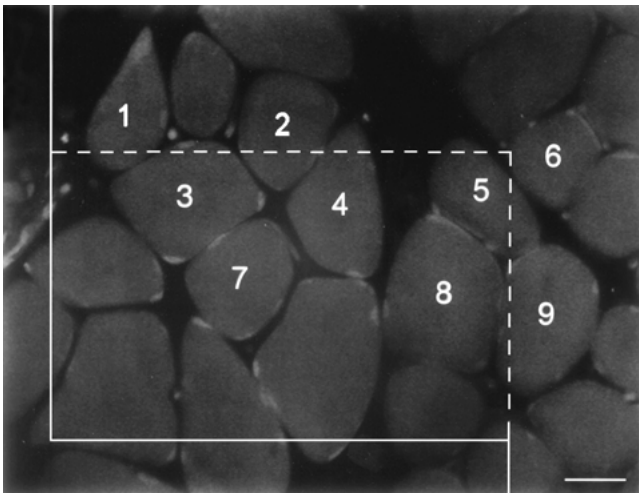

Fig. 2. Sampling fibres by unbiased sampling frame. Fibres with the profiles lying at least partly in the frame, and not intersected by the full (forbidden) line, are sampled for the measurement. Nine fibres are sampled here. Scale bar equals 30 μm.

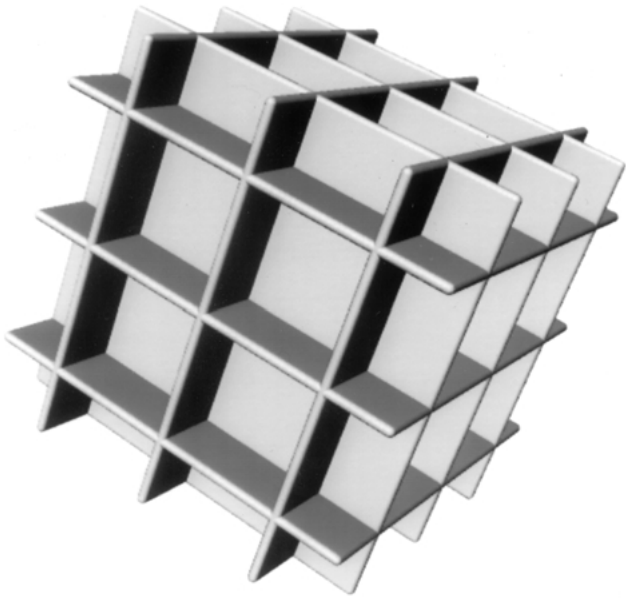

Fig. 3. Cubic, spatial grid consisting of three mutually perpendicular SLICER probes. For the sake of clarity, the test planes are shown as 'boards' here.

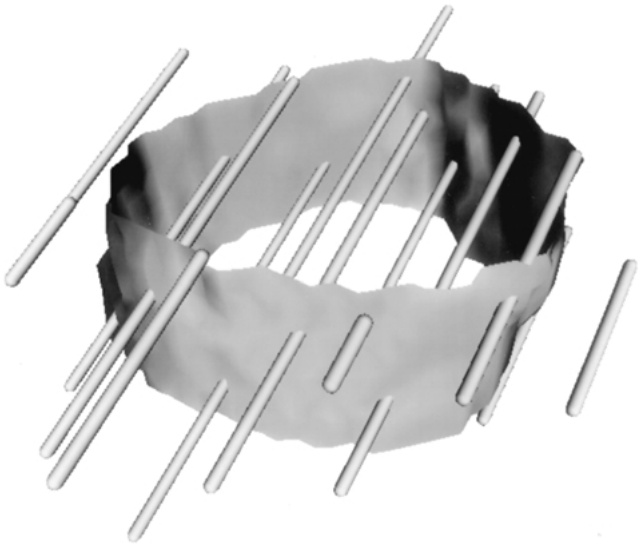

Fig. 4. FAKIR probe piercing the muscle fibre. To estimate the fibre surface area, the intersections between the test lines and the fibre surface are counted. For the sake of clarity, the test lines are shown as 'pipes' here.

superimposed on the image of the first section of the stack (Figure 2) using the STESYS software system (Karen *et al.*, 1998; Tomori *et al.*, 2000). A drawing or print of the section was made and each sampled fibre was marked by a number for its clear identification during all different measurements (Figure 2). Capillaries supplying a specific muscle fibre were defined as adjacent capillaries. A capillary was classified as an adjacent capillary if its wall was at a distance of 5 μm or less from a muscle fibre wall. Therefore, the same capillary could supply several muscle fibres.

Each sampled fibre and adjacent capillaries were evaluated as follows:

(1) The length of capillaries adjacent to the ith fibre in the given stack (L_i(cap)) was estimated by the 'slicer' method (called 'global spatial sampling' by Larsen *et al.*, 1998). The SLICER probe is a systematic probe consisting of parallel equidistant test planes. When estimating the capillary length, the intersections between the isotropic virtual test planes (generated by a computer using a procedure described in Appendix A3 in Cruz-Orive, 1997) and the capillaries adjacent to the ith fibre lying in the stack are counted.

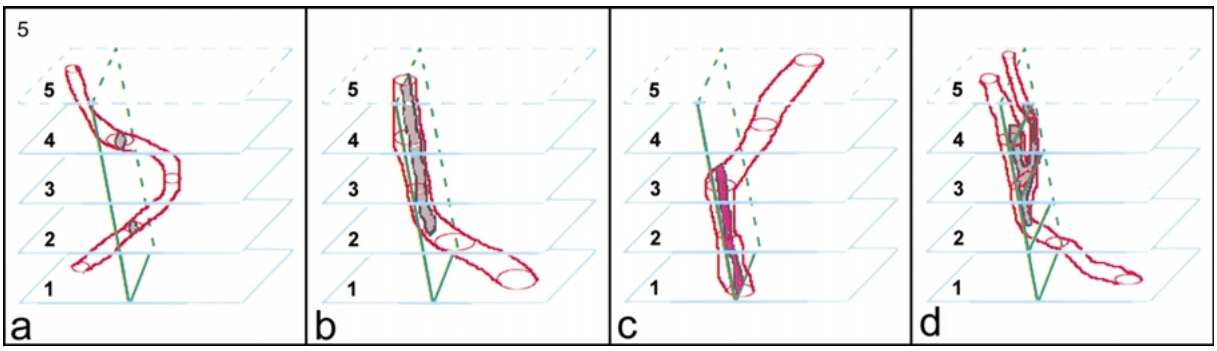

Fig. 5. Counting intersections between capillaries and SLICER probes. Stacks of five serial optical sections (light blue, numbered 1–5) containing a capillary (red) intersected by a SLICER test plane (green) are shown here. For unbiased counting of intersections, the first (number 1), lowest section of the stack has to be 'forbidden', i.e. if the intersection is present in this section, it is not counted. (a) Two intersections (grey, in optical sections 2 and 4) are counted here as both are lying inside the stack. (b) One intersection (grey, spanning optical sections 3, 4 and 5) is counted, although it is not entirely inside the stack, because it is not present in the first, 'forbidden' section. (c) No intersection is counted, as the intersection (violet) is also present in the 'forbidden', optical section 1. (d) One intersection (grey) is counted for this branching capillary, as it is really only one, although two capillary profiles are seen in the fourth optical section.

We have used a cubic spatial grid consisting of three mutually perpendicular SLICER probes (Figure 3). In this case the length of capillaries adjacent to the *i*th fibre in the given stack (L_i(cap)) can be estimated by the following formula:

$$\mathrm{est}L_i(\mathrm{cap}) = \tfrac{2}{3}d(Q_1^i + Q_2^i + Q_3^i), \qquad (1)$$

where d is the distance between neighboring parallel planes, Q_j^i ($j = 1,2,3$) is the number of intersections between the jth SLICER probe and the capillaries adjacent to the ith fibre within the given stack. This estimator of the length is unbiased if the orientation of the spatial grid of planes is isotropic and the intersections are counted properly (see Larsen *et al.*, 1998 and Figure 5). The distance (d) between SLICER planes was chosen to be 10 μm for both types of muscles ensuring about 20–50 intersections per fibre.

The measurement was easily performed using our interactive SLICER software (written in TurboPascal 6 for IBM PC under MS DOS). This software generates an isotropic spatial grid of planes and so it is not necessary to randomize the direction of the stack of sections, which means that the thick transverse muscle sections can be used. The software enables to browse not only through the optical sections in *xy* direction (i.e. parallel to the plane of observation) but also through those in the *xz* and *yz* directions (perpendicular to the plane of observation) so that it is possible to check if the capillary course was detected correctly (see Figure 6).

(2) The number of capillary branchings adjacent to the *i*th fibre (N_i(branch)) in the given stack were counted during the above measurement using the SLICER software for browsing through the stack. The branching of capillaries was detected if two capillary profiles in one optical section joined into one profile in the successive section, or vice versa, i.e. if one capillary profile, seen in one section, was disconnected into two profiles in the consecutive optical section. The correct detection of capillary branchings was checked in *xz* and *yz* directions. Only the capillary branchings in the 5 μm proximity of the *i*th fibre were counted.

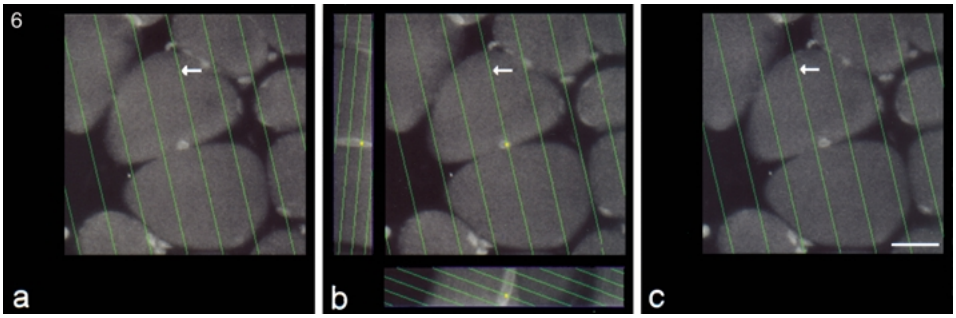

Fig. 6. Using SLICER software for estimating the length of capillaries adjacent to the fibre. The optical sections within a thick muscle slice are browsed through with the (green) SLICER probe applied. During browsing (i.e. focussing), the green lines (showing the intersection between the SLICER test planes and the current optical section) are moving. The white arrows point at one of the SLICER planes intersecting a capillary. The intersection is marked as a yellow point by a mouse. (a) Lower optical section. (b) Middle optical section with the capillary intersection. Together with the lateral (*xy*) view also the orthogonal (*xz*, *yz*) views going through the yellow point of intersection are shown. (c) Upper optical section. Scale bar equals 20 μm.

(3) The surface area of the ith fibre in the given stack (S_i(fib)) was estimated by FAKIR method (Kubínová and Janáček, 1998) using FAKIR probes. The FAKIR probe (named by Cruz-Orive, 1993) is a spatial grid of lines consisting of parallel test lines (resembling nails of a fakir bed piercing the surface, see Figure 4).

When estimating the fibre surface area, the intersections between the fibre surface and the FAKIR probe are counted. In our study we have used a cubic spatial grid consisting of three mutually perpendicular FAKIR probes, halfway shifted with respect to each other (Figure 2 in Kubínová and Janáček, 1998) which has been proved to be highly efficient. In this case the surface area of the ith fibre in the stack (S_i(fib)) can be estimated by the following formula:

$$\mathrm{est}S_i(\mathrm{fib}) = \tfrac{2}{3}u^2(I_1^i + I_2^i + I_3^i), \tag{2}$$

where u is the grid constant (i.e. distance between neighboring parallel lines of the grid), I_j^i $(j = 1, 2, 3)$ is the number of intersections between the jth probe and the ith fibre surface lying in the stack. This estimator of the surface area is unbiased if the orientation of the spatial grid is isotropic.

The measurement was easily performed using our interactive FAKIR software (written in TurboPascal 6 for IBM PC under MS DOS). This software generates an isotropic set of FAKIR probes (Figure 7) and so it is not necessary to randomize the direction of the stack of sections which means that the thick transverse muscle sections can be used. The grid constant was chosen to be 15 μm for EDL muscle fibres and 20 μm for SOL fibres ensuring on average about 40 intersections per fibre.

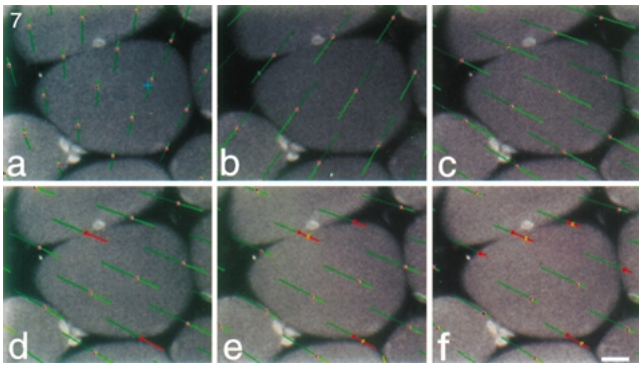

Fig. 7. Using the FAKIR software for estimating the surface area of the fibre within the muscle slice. An isotropic set of three mutually perpendicular FAKIR probes is generated as shown in (a), (b), and (c). The green lines are the FAKIR test lines within the muscle slice, the violet squares denote the intersection points between the test lines and the current optical section. The procedure during counting of intersection points between the test line and the fibre surface area is shown in (c), (d), (e), and (f): The optical sections are browsed through with the FAKIR probe applied. During browsing, the violet squares are moving along the test lines. (c) First section. (d) Second section showing two intersection points marked red by a mouse. (e) Third section showing the next intersection point (marked red). The yellow squares denote the intersection points between the displayed optical section and the test lines already having intersected the fibre surface area. (f) Fourth section showing the last two intersection points (marked red). Scale bar equals 10 μm.

(4) The length of the ith fibre in the stack (L_i(fib)): As the fibres are perpendicular to the direction of sectioning, their length in a stack is equal to its thickness, which was 40 μm in our case, and so:

$$L_i(\mathrm{fib}) = 40\,\mu\mathrm{m}. \tag{3}$$

(5) The volume of the ith fibre in the given stack (V_i(fib)) was estimated using the spatial grid of points (Cruz-Orive, 1997) which is a modification of the Cavalieri principle (Gundersen and Jensen, 1987). The Cavalieri principle is a stereological method for estimating the object volume by summing up the areas of systematic parallel sections of the object and multiplying this sum by the distance between two neighboring sections. The position of the first section should be uniform random. The section area is usually estimated by point counting, i.e. a point grid is superimposed on each section and the number of points falling into the section is counted. In our case, when a cubic spatial grid of points was used, the volume (V_i(fib)) was estimated by the following formula:

$$\mathrm{est}V_i(\mathrm{fib}) = T(u')^2 \sum_{j=1}^{n} P_{ij}(\mathrm{fib}), \tag{4}$$

where T is the distance between sections, u' is the distance between two neighboring points in the grid, and P_{ij} $(j = 1, 2, \ldots, \mathrm{n})$ is the number of test points falling in the jth section of the ith fibre. In our case the distance T between sections as well as the grid constant u' was chosen to be 10 μm for both types of muscle fibres ensuring about 50–100 points hitting the fibre.

The above method was implemented using the SANDAU program (written in TurboPascal 6 for IBM PC under MS DOS) generating a square point grid and superimposing it on sections. The test points (given by the knot points of the test grid) falling into the fibre profile in the parallel systematic optical sections were then counted.

After all above measurements of sampled fibres and adjacent capillaries within the 40 μm thick muscle slices were performed, the following parameters could be estimated for each muscle under study:

(a) Mean fibre surface area within the muscle slice (S(fib))
(b) Mean fibre volume within the muscle slice (V(fib))
(c) Mean length of capillaries adjacent to a fibre within the muscle slice (L(cap))
(d) Mean capillary length/adjacent fibre surface area (L(cap)/S(fib))
(e) Mean capillary length/adjacent fibre length (L(cap)/L(fib))
(f) Mean capillary length/adjacent fibre volume (L(cap)/V(fib))
(g) Mean number of capillary branchings adjacent to a fibre within the muscle slice (N(branch))

(h) Mean number of capillary branchings/capillary length (N(branch)/L(cap))

For the control of possible deformation of muscle fibres during the tissue processing, the mean sarcomere length was measured under the confocal microscope from longitudinal muscle sections using the Paint Shop Pro (Jasc Software Inc., USA) software.

3D reconstructions

One stack of about 80 serial sections encompassing a $300 \times 200 \times 80$ μm^3 volume of tissue was taken from each muscle slice. It served for the surface rendering of capillaries and fibres using an interactive custom-made CutView programme (Jirák *et al*., 1997) running on PC (when the contours of muscle fibres and capillaries were manually delineated using a digitization tablet) and using the IRIS Explorer visualization system (SGI, USA) running on an INDY (SGI, USA) graphical workstation and supplemented with custom-made modules for volume data processing.

Results

3D reconstructions

Computer generated 3D images of muscle fibres suggest that SOL fibres have a larger diameter and more capillaries per fibre than EDL (Figure 8).

The 3D reconstruction of one fibre and its adjacent capillaries took more than 10 h and so the capillary network of only a few muscle fibres could be visualized.

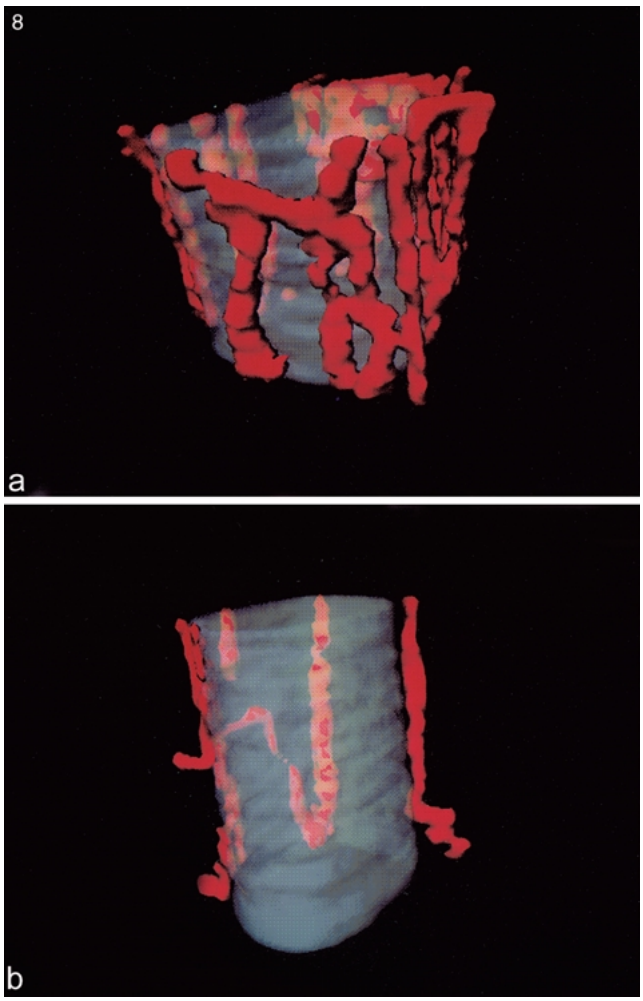

Fig. 8. Computer generated, 3D reconstruction of a typical SOL (Figure 8a, fibre length equals 70 μm, fibre diameter is approximately 60 μm) and EDL (Figure 8b, fibre length equals 80 μm, fibre diameter is approximately 50 μm) muscle fibre with adjacent capillaries.

Stereological measurements

The above observations are supported by statistical comparisons between EDL and SOL of muscle fibre surface area, muscle fibre volume, and capillary length (Table 1). SOL had a statistically significant larger muscle fibre surface area ($P = 0.002$), muscle fibre volume ($P = 0.006$), number of capillary branchings per fibre ($P = 0.012$), and length of capillaries per fibre length ($P = 0.006$). There was no significant difference between EDL and SOL in the mean capillary length/adjacent fibre surface area, the mean capillary length/adjacent fibre volume and the number of capillary branchings per capillary length. The sarcomere length varied from 2.2 to 2.7 μm for SOL and from 2.1 to 2.2 μm for EDL muscles.

The measurement of the length of capillaries adjacent to one fibre together with counting capillary branchings took 15–25 min, depending on the complexity of the course of capillaries. It took about 4 min to estimate the fibre surface area and only 1 min to measure its volume. In summary, the measurements of all above parameters took 20–30 min per fibre. Fibres were analysed in five EDL and five SOL muscles (one EDL and one SOL per animal). On average 33 fibres were evaluated per EDL muscle and 19 fibres per SOL muscle.

Discussion

Our study points to statistically significant differences between EDL and SOL muscle in the length of capillaries and in the number of capillary branchings adjacent to a fibre. Both parameters had higher values in SOL compared to EDL muscle. This observation is consistent with previous reports based on 2D analysis (Mai *et al*., 1970; Brown *et al*., 1976) concluding that slow muscles (i.e. SOL) have a larger number of capillaries per muscle fibre than fast muscles (i.e. EDL). However, a larger capillary length (or number) per muscle fibre does not necessarily mean a better blood supply. The quality of a fibre's blood supply depends not only on the number of its capillaries but, among other things, also on the ratio of capillary length to fibre volume and surface area. There was no statistically significant difference in ratios of capillary

Table 1. Morphometric characteristics of muscle fibres and capillaries in the rat EDL and SOL muscles within 40 μm thick muscle slice (mean ± SD)

	EDL	SOL	EDL:SOL
S(fib) (μm^2)	5246 ± 445	7060 ± 767	$P = 0.002$
V(fib) (μm^3)	50080 ± 10160	85280 ± 18321	$P = 0.006$
L(cap) (μm)	152 ± 15	230 ± 44	$P = 0.005$
L(cap)/S(fib) (μm^{-1})	0.0309 ± 0.005	0.0341 ± 0.008	NS ($P = 0.474$)
L(cap)/L(fib)	3.808 ± 0.38	5.772 ± 1.103	$P = 0.005$
L(cap)/V(fib) (mm^{-2})	3708 ± 873	2884 ± 829	NS ($P = 0.165$)
N(branch)	1.072 ± 0.149	2.450 ± 0.942	$P = 0.012$
N(branch)/L(cap) (μm^{-1})	0.007 ± 0.0007	0.0106 ± 0.0053	NS ($P = 0.12$)

Comparisons between EDL and SOL (EDL:SOL) were made with the unpaired, two-tailed, Student t-test. (NS – not statistically significant, $P > 0.05$). (S(fib)) – muscle fibre surface area; (V(fib)) – muscle fibre volume; (L(cap)) – length of capillaries adjacent to a fibre; (L(cap)/S(fib)) – capillary length to adjacent fibre surface area; (L(cap)/L(fib)) – capillary length to adjacent fibre length; (L(cap)/V(fib)) – capillary length to adjacent fibre volume; (N(branch)) – number of capillary branchings adjacent to a fibre; (N(branch)/L(cap)) – number of capillary branchings to capillary length.

length to fibre surface area (L(cap)/S(fib)) and capillary length to fibre volume (L(cap)/V(fib)) between these two types of muscles (Table 1).

In our study, tissue samples were excised in the middle of the muscle belly of both SOL and EDL muscles where vascular supply was reported as the most scarce (Williams and Segal, 1992). Therefore, we assume that differences in the fibre capillary network could be even larger if muscle samples were taken from different portions of both muscles. Additionally, it can be assumed that larger differences in capillary supply between SOL and EDL could be obtained if we evaluated capillary supply separately for fibre types since EDL has a heterogeneous population of muscle fibres (Pullen, 1977; Egginton, 1990). SOL is a homogeneous, slow twitch muscle with muscle fibres of average volume and surface area larger than in EDL muscle. Very rare fast twitch fibres in SOL are always of type 2a. EDL muscle, however, is a fast twitch muscle containing scarce slow twitch fibres and a heterogeneous population of fast twitch fibres (2a, 2x/d and 2b) with a span of fibre diameters from the smallest (2a and 1) to the largest (2b) (Pullen, 1977; Schiaffino *et al.*, 1989; Gorza, 1990). The density of the capillary network is in positive correlation with the oxidative enzyme activity. The smallest fibres (2a and type 1) in the EDL are predominantly oxidative as shown by the activity of SDH or NADH compared to 2b fibres which are predominantly glycolytic. Type 1 fibres in SOL, though much more numerous than in EDL, are less oxidative than type 1 fibres in EDL muscle (Punkt *et al.*, 1996). Consequently, citrate synthase activity, when measured from whole muscle homogenates, does not exhibit any differences between both muscles (Bass *et al.*, 1983; Kriketos *et al.*, 1995).

In our model, only capillaries lying at the distance of 5 μm or less from a muscle fibre boundary were assumed to be supplying a muscle fibre. The choice of this 5 μm limit was based on the data on capillary diameter and oxygen diffusion distances from capillary to muscle fibre. The outer diameters of muscle fibre capillaries range from 4–15 μm and muscle fibres receive oxygen by diffusion from capillaries across an average distance of 50 μm during rest and only a few micrometers during work (Jerusalem, 1994). The approach we have used permits to measure fibre diameter as well, however, tissue pretreatment and detection of capillaries by fluorescent markers can be an evident source of error.

In our study muscles were fixed by immersion. Consequently, it could be expected for our muscle samples to have shorter sarcomere length, in comparison with the perfusion fixed muscles, as well as a variable degree of muscle fibre kinking, collaps of capillary wall and diminished degree of anisotropy of capillaries (Mathieu *et al.*, 1983). Due to many collapsed capillaries, an unbiased estimation of the diameter and capillary volume was not possible. Though the present study would allow to use the more suitable perfusion fixation, we chose fixation by immersion on purpose: the stereological methods that we are developing should namely be applicable also on biopsy samples where fixation by perfusion is not feasible.

We are aware that in immersion-fixed muscles, there can be a more pronounced tortuousity of capillaries which then leads to an overestimation of their length density. It is known that the capillary tortuosity increases with muscle contraction (Ranvier, 1874; Krogh, 1919), therefore a correction of the bias of the length density measurement can be obtained if sarcomere length is taken into account (Mathieu-Costello, 1987). As long as capillaries are in a tortuous configuration, muscle extension will merely decrease the tortuosity, leaving vessel length unaltered (Ellis *et al.*, 1990). Further extension of the muscle will cause the vessels to stretch. By means of intravital videomicroscopy Ellis *et al.* (1990) have demonstrated that stretching of individual capillaries does indeed occur over a sarcomere length range of 2.1–2.9 μm in rat extensor digitorum longus muscle. In our muscle samples, the sarcomere length ranged from 2.1 to 2.7 μm. SOL muscles were more stretched than EDL (average sarcomere length in SOL 2.5 vs. 2.2 μm in EDL). However, in both muscles, the sarcomere length within this range

(Ellis *et al*., 1990) should not influence tortuosity. Therefore, it was not necessary to do any corrections for capillary stretching.

Parameters L(cap)/V(fib), L(cap)/S(fib) and L(cap)/L(fib) that we measured in 3D correspond to some extent to N(cap)/A(fib) (number of capillary profiles per fibre profile area), N(cap)/B(fib) (number of capillary profiles per fibre perimeter) and N(cap)/N(fib) (number of capillary profiles per fibre), i.e. the capillary to fibre ratio, all measured in 2D. Though different additional parameters have been introduced to study capillary supply in 2D, the capillary to fibre ratio still remains the most often used parameter, related to L(cap)/L(fib), which gives information that does not depend on fibre diameter nor on the fibre number. However, if the sections have a fixed, specific orientation (e.g. perpendicular to the muscle main axis), the number of capillary profiles (N(cap)) is not, in general, in an unambigous relationship with the capillary length due to different capillary tortuosity and existence of transverse capillaries. It is thus more relevant to estimate the capillary length directly as it was done in our study. Which parameter describes the capillary network most efficiently in regard to its physiological properties, still remains an open question.

Our study showed that the 3D approach to the evaluation of muscle fibre capillarization brings many advantages over the traditional measurements in 2D:

(1) We have measured, in an unbiased way, the actual length of capillary network, distributed in 3D space, which should be more relevant from the functional point of view than the number of capillary profiles counted in transverse muscle sections. In principle, the length of capillaries can be estimated also from single physical sections by other stereological methods (for overview see Hudlicka *et al*., 1992), e.g. design-based methods using vertical slices (Gokhale, 1990) or orientator (Mattfeldt *et al*., 1990). However, in these methods, the section orientation must be randomized (i.e. transverse sections cannot be used) which is more tedious than randomizing virtual test probes. Moreover, it is easier to recognize the capillaries within stacks of optical sections than recognizing capillary profiles in randomized sections, as the option to view in *xy*, *xz* and *yz* directions is available in our measurements. It should be stressed here that optical sections of thickness less than 1 μm are evaluated here, therefore, the overprojection problems are far less pronounced than in stereological methods based on measurements of one, several micrometers thick physical section.

(2) It was possible to get an idea about the topology and course of capillaries adjacent to individual muscle fibres. The number of capillary branchings can be easily and directly counted. During focussing through the capillary network, it was possible also to examine the course of capillaries and it was clear that, although some capillaries are going almost parallel with the fibres, many capillaries are curling round the fibres while other ones form short transverse connections between longer capillaries. There was no statistically significant difference in the number of capillary branchings to capillary length between EDL and SOL fibres. This would suggest that both muscles do not have, on average, significantly different density of capillary network of individual fibres.

(3) 3D reconstructions of selected fibres and their capillary network made it possible to visualize the capillary topography (connections between capillaries and tortuosity of capillaries) that could be viewed from different angles. This possibility also enables the user to verify the accuracy of locating capillaries on 2D images of muscle tissue. Incorrectly marked or omitted capillaries lead to computer generated 3D images of capillaries with discontinuities (Figure 9).

For 3D reconstruction of capillaries, we have used images of perfectly registered optical sections recorded by a confocal microscope. A similar method proved to be suitable also for visualization of the capillary bed of a placental terminal villus (Jirkovská *et al*., 1998). Confocal microscopy was also used for 3D reconstruction of glomerular capillaries by Kaczmarek (1999) who tried to apply methods for automatic capillary segmentation which was not feasible in our case. There are many other methods that may be used for the study of the vascular arrangement of a skeletal muscle. Corrosion methods of perfused muscles allow spatial reconstruction of the vascular network but without any information on surrounding tissue (Potter and Groom, 1983). However, in order to reveal the biological role of capillaries, it is desirable to study the 3D distribution of capillary network in relation to skeletal muscle tissue. The methods of injection can cause artificial changes of blood vessels like reactive constriction (Aharinejad *et al*., 1993) and there is also a danger that all capillaries are not perfused (Kondering *et al*., 1992). Vital microscopy has been found to be suitable for measurements of vessel dimensions (Baez, 1969) but the method can be applied only for experimental purposes and can visualize

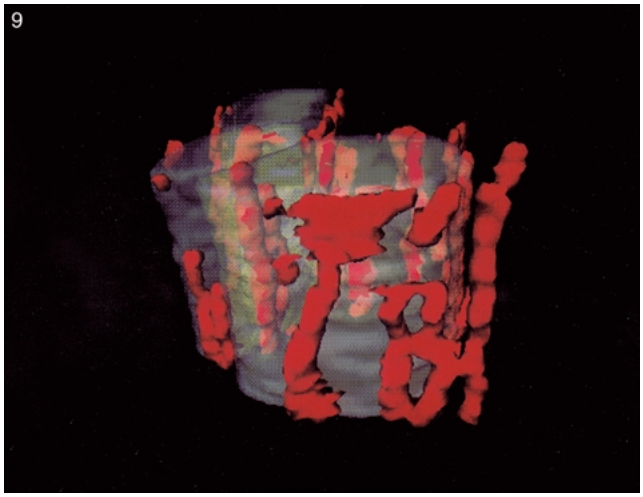

Fig. 9. Computer generated, 3D reconstruction of muscle fibres with incorrectly marked adjacent capillaries. The fibre in front is the same as in Figure 8a. Note the resulting discontinuities.

vascular network only within thin muscles (Myrhage, 1977). To our knowledge, the quantitative analyses of capillary geometry were done only in 2D from the video monitor or from the acetate paper tracing (Kinding *et al*., 1998). The whole-mount lectin technique is used to visualize the pattern of capillaries but is also applicable only to quite thin muscles such as hamster cheek pouch, mouse diaphragm, rat cremaster (Hansen-Smith *et al*., 1988) and *extensor hallucis proprius* (EHP) muscle (Hansen-Smith *et al*., 1996).

(4) In the present study, we have not evaluated the local capillary supply to muscles, usually based on measuring the area of tissue surrounding the given capillary in a muscle transverse section (Hoofd *et al*., 1985; Egginton and Ross, 1989b). Even here it would be interesting to apply a 3D approach, using 3D image data from our study, when the volume of 3D domains in the neighborhood of single capillaries would be measured.

The methods presented in this paper are relatively time consuming. The rate limiting step is very often a tedious identification of capillaries which requires to look at the same structure in *xy*, *xz* and *yz* plane. To speed up this step, a better staining is needed which would meet the following requirements: it should be more specific which subsequently will provide a good contrast between capillaries and other components of the muscle tissue, it should penetrate sufficiently deep into the tissue and fluorescent detection would be necessary. Possible candidates which seem to be appropriate are CD31 or laminin in combination with von Willebrand factor.

During angiogenesis, new capillary blood vessels generate from existent microvessels by sprouting. Angiogenesis is a morphogenetic process that plays a major role in the evolvement of a vascular supply in adult tissue remodeling and disease (Battegay, 1995). The methodology described in this study enables unbiased quantification of capillary branching as a response to increased expression of angiogenic molecules, like, for example, vascular endothelial growth factor (VEGF), platelet derived growth factor (PDGF) and transforming growth factor-β_1 (TGF-β_1) (for review see Battegay, 1995). An adequate capillary network is essential for tissue survival. Therefore, 3D quantification of capillary supply could be a useful tool to evaluate angiogenesis, for example, during tumor growth (Folkman, 1995), ischemic heart disease (Schaper *et al*., 1988; Schaper *et al*., 1990) and diabetic neuropathy (Frank, 1994).

Acknowledgements

This study was supported by the Ministry of Science and Technology of Slovenia and the Ministry of Education, Youth and Sport of the Czech Republic (KONTAKT grant no. 256/98), the Grant Agency of the Academy of Sciences of the Czech Republic (grant no. A5011810) and the Grant Agency of the Czech Republic (grant no. 304/01/0257).

References

Aharinejad S, McDonald IC, Mackay CE and Masonsavas A (1993) New aspects of microvascular corrosion casting – a scanning, transmission electron and high resolution intravital video microscopic study. *Microsc Res Tech* **26:** 473–488.

Amann K, Breitbach M, Ritz E and Mall G (1998) Myocyte/capillary mismatch in the heart of uremic patients. *J Am Soc Nephrol* **9:** 1018–1022.

Anversa P, Capasso JM, Ricci R, Sonnenblick EH and Olivetti G (1989) Morphometric analysis of coronary capillaries during physiologic myocardial growth and induced cardiac hypertrophy: a review. *Int J Microcirc Clin Exp* **8:** 353–363.

Artacho-Perula E and Roldan-Villalobos R (1995) Estimation of capillary length density in skeletal muscle by unbiased stereological methods: I. use of vertical slices of known thickness. *Anat Rec* **241:** 337–344.

Baez S (1969) Simultaenous measurements of radii and wall thickness of microvessels in the anaesthetized rat. *Circ Res* **25:** 315–329.

Bass A, Teisinger J, Hnik P, Mackova E, Vejsada R and Erzen I (1983) Changes of lysosomal and energy-supply enzymes in hypertrophying muscles after denervation. *Physiologia Bohemoslovaca* **32:** 506.

Batra S, Konig MF and Cruz-Orive LM (1995) Unbiased estimation of capillary length from vertical slices. *J Microsc* **178:** 152–159.

Battegay EJ (1995) Angiogenesis: mechanistic insights, neovascular diseases and therapeutic prospects. *J Mol Med* **73:** 333–346.

Brodal P, Ingjer F and Hermansen L (1977) Capillary supply of skeletal muscle fibres in untrained and endurance-trained men. *Am J Physiol* **232:** H705–H712.

Brown MD, Cotter MA, Hudlická O and Vrbová G (1976) The effects of different pattern of muscle activity on capillary density, mechanical properties and structure of slow and fast rabbit muscles. *Pflüg Arch* **361:** 241–250.

Cruz-Orive LM (1993) Systematic sampling in stereology. *Bull Intern Statis Inst Proceedings 49th Session, Florence 1993* **55(2):** 451–468.

Cruz-Orive LM (1997) Stereology of single objects. *J Microsc* **186:** 93–107.

Egginton S (1987) Effect of an anabolic hormone on aerobic capacity of rat striated muscle. *Pflüg Arch* **410:** 356–361.

Egginton S (1990). Numerical and areal density estimates of fibre type composition in a skeletal muscle (rat extensor digitorum longus). *J Anat* **168:** 73–80.

Egginton S and Ross HF (1989a) Quantifying capillary distribution in four dimensions. *Adv Exp Med Biol* **248:** 271–280.

Egginton S and Ross HF (1989b) Influence of muscle phenotype on local capillary supply. *Adv Exp Med Biol* **248:** 281–291.

Egginton S, Turek Z and Hoofd L (1987) Morphometric analysis of sparse capillary networks. *Adv Exp Med Biol* **215:** 1–12.

Eken T and Gundersen K (1988) Electrical stimulation resembling normal motor-unit activity: effects on denervated fast and slow rat muscles. *J Physiol* **402:** 651–669.

Ellis CG, Mathieu-Costello O, Potter RF, MacDonald IC and Groom AC (1990) Effect of sarcomere length on total capillary length in skeletal muscle: in vivo evidence for longitudinal stretching of capillaries. *Microvasc Res* **40:** 63–72.

Endre T, Mattiasson I, Berglund G and Hulthen UL (1998) Muscle fibre composition and glycogen synthase activity in hypertension-prone men. *J Int Med* **243:** 141–147.

Eržen I and Maravić V (1993) Simultaneous histochemical demonstration of capillaries and muscle fibre types. *Histochemistry* **99:** 57–60.

Folkman J (1995) Angiogenesis in cancer, vascular, rheumatoid and other disease. *Nature Med* **1:** 27–31.

Folkman J and D'Amore PA (1996) Blood vessel formation: what is its molecular basis. *Cell* **87:** 1153–1155.

Frank RM (1994) Vascular endothelial growth factor-its role in retinal vascular proliferation. *N Engl J Med* **331:** 1519–1520.

Gokhale AM (1990) Unbiased estimation of curve length in 3D using vertical slices. *J Microsc* **159:** 133–141.

Gorza L (1990) Identification of a novel type 2 fiber population in mammalian skeletal muscle by combined use of histochemical

myosin ATPase and anti-myosin monoclonal antibodies. *J Histochem Cytochem* **38:** 257–265.

Gray SD and Renkin EM (1978) Microvascular supply in relation to fibre metabolic type in mixed skeletal muscles of rabbits. *Microvasc Res* **16:** 406–425.

Green H, Goreham C, Ouyang J, Ball-Burnett M and Ranney D (1999) Regulation of fibre size, oxidative potential, and capillarization in human muscle by resistance exercise. *Am J Physiol* **276:** R591–R596.

Gundersen HJG (1977) Notes on the estimation of the numerical density of arbitrary profiles: the edge effect. *J Microsc* **111:** 219–223.

Gundersen HJG and Jensen EB (1987) The efficiency of systematic sampling in stereology and its prediction. *J Microsc* **147:** 229–263.

Hansen-Smith FM, Watson L and Lu DY (1988) Griffonia simplicifoila I: fluorescent tracer for microcirculatory vessels in nonperfused thin muscles and sectioned muscle. *Microvasc Res* **36(3):** 199–215.

Hansen-Smith FM, Hudlicka O and Egginton S (1996) In vivo angiogenesis in adult rat skeletal muscle: early changes in capillary network architecture and ultrastructure. *Cell Tisue Res* **286:** 123–136.

Hernandez N, Torres SH, Finol HJ, Sosa A and Cierco M (1996) Capillary and muscle fibre type changes in DOCA-salt hypertensive rats. *Anatomical Record* **246:** 208–216.

Hoofd L, Turek Z, Kubat K, Ringnalda BEM and Kazda S (1985) Variability of intercapillary distance estimated on histological sections of rat heart. *Adv Exp Biol* **191:** 239–297.

Hudlicka O (1991) What makes blood vessels grow? *J Physiol* **444:** 1–24.

Hudlicka O, Brown M and Egginton S (1992) Angiogenesis in skeletal and cardiac muscle. *Physiol Rev* **72:** 369–417.

Ingjer F (1979) Effects of endurance training on muscle fibre ATP-ase activity, capillary supply and mitochondrial content in man. *J Physiol* **294:** 419–432.

Isner JM, Baumgartner I, Rauh G, Schainfeld R, Blair R, Manor O, Razvi S and Symes JF (1998) Treatment of thromboangiitis obliterans (Buerger's disease) by intramuscular gene transfer of vascular endothelial growth factor: preliminary clinical results. *J Vascular Surg* **28:** 964–973.

James NT (1981) A stereological analysis of capillaries in normal and hypertrophic muscle. *J Morphol* **168:** 43–49.

Jerusalem F (1994) The microcirculation of muscle. In: Engel AG and Franzini-Armstrong C (eds) *Myology*. (vol. 1, p. 368) McGraw-Hill, New York.

Jirák D, Kubínová L, Tomori Z, Hlinka R, Jirkovská M and Krekule I (1997) Interactive visualization of a capillary bed. *Physiol Res* **46:** 33.

Jirkovská M, Kubínová L, Krekule I and Hach P (1998) Spatial arrangement of fetal placental capillaries in terminal villi: a study using confocal microscopy. *Anat Embryol* **197:** 263–272.

Kaczmarek E (1999) Visualisation and modelling of renal capillaries from confocal images. *Med Biol Eng Comput* **37:** 273–277.

Karen P, Kubínová L and Krekule I (1998) STESYS software for computer-assisted stereology. *Physiol Res* **47:** 271–278.

Kinding CA, Sexton WL, Fedde MR and Poole DC (1998) Skeletal muscle microcirculatory structure and hemodynamics in diabetes. *Resp Physiol* **111:** 163–175.

Kondering MA, van Ackern C, Steinberg F and Streffer CH (1992) Combined morphological approaches in the study of network formation in tumor angiogenesis. In: Steiner R, Weisz PB and Langer R, (eds) *Angiogenesis: Key Principles–Science–Technology–Medicine*. Birkauser Verlag, Basel, 40–58.

Koyama T, Gao M, Batra S, Togashi H and Saito H (1997) Myocyte hypertrophy and capillarization in spontaneously hypertensive stroke-prone rats. *Adv Exp Med Biol* **411:** 365–368.

Kriketos AD, Pan DA, Sutton JR, Hoh JFY, Baur LA, Cooney GJ, Jenkins AB and Storlien LH (1995) Relationships between muscle membrane lipids, fiber type and enzyme activities in sedentary and exercised rats. *Am J Physiol* **269** (*Regulatory Integrative Comp Physiol* **38**)**:** R1154–R1162.

Krogh A (1919) The number and distribution of capillaries in muscles with calculations of the oxygen pressure head necessary for supplying the tissue. *J Physiol* **52:** 409–415.

Kubínová L and Janáček J (1998) Estimating surface area by isotropic fakir method from thick slices cut in arbitrary direction. *J Microsc* **191:** 201–211.

Large J and Tyler KR (1985) Changes in capillary distribution in rat fast muscles following nerve crush and reinnervation. *J Physiol* **362:** 13–21.

Larsen JO, Gundersen HJG and Nielsen J (1998) Global spatial sampling with isotropic virtual planes: estimators of length density and total length in thick, arbitrarily orientated sections. *J Microsc* **191:** 238–248.

Mai JV, Edgerton VR and Barnard RJ (1970) Capillarity of red, white and intermediate muscle fibres in trained and untrained guinea-pigs. *Experientia* **26:** 1222–1223.

Mall G, Schikora I, Mattfeldt T and Bodle R (1987) Dipyridamole-induced neoformation of capillaries in the rat heart. Quantitative stereological study on papillary muscles. *Lab Invest* **57:** 86–93.

Mathieu O, Cruz-Orive LM, Hoppeler H and Weibel ER (1983) Estimating length density and quantifying anisotropy in skeletal muscle capillaries. *J Microsc* **131:** 131–146.

Mathieu-Costello O (1987) Capillary tortuosity and degree of contraction or extension of skeletal muscles. *Microvasc Res* **33:** 98–117.

Mathieu-Costello O (1994) Morphometry of the size of the capillary-to-fiber interface in muscles. *Adv Exp Med Biol* **345:** 661–668.

Mathieu-Costello O, Potter RF, Ellis CG and Groom AC (1988) Capillary configuration and fiber shortening in muscles of the rat hindlimb: correlation between corrosion casts and stereological measurements. *Microvasc Res* **36:** 40–55.

Mattfeldt T, Möbius H-J and Mall G (1985) Orthogonal triplet probes; an efficient method for unbiased estimation of length and surface of objects with unknown orientation in space. *J Microsc* **139:** 279–289.

Mattfeldt T, Mall G, Gharehbaghi H and Moller P (1990) Estimation of surface area and length with the orientator. *J Microsc* **159:** 301–317.

McMillan PJ, Archambeau JO, Gokhale AM, Archambeau M-H and Oey M (1994) Morphometric and stereologic analysis of cerebral cortical microvessels using opical sections and thin slices. *Acta Stereol* **13:** 33–38.

Murakami H, Yayama K, Miao RQ, Wang C, Chao L and Chao J (1999) Kallikrein gene delivery inhibits vascular smooth muscle cell growth and neointima formation in the rat artery after balloon angioplasty. *Hypertension* **34:** 164–170.

Myrhage R (1977) Microvascular supply of skeletal muscle fibres. *Acta Orthopaed Scan* **168** (Suppl)**:** 1–46.

Nyengaard JR and Gundersen HJG (1992) The isector: a simple and direct method for generating isotropic, uniform random sections from small specimens. *J Microsc* **158:** 19–30.

Nyholm B, Qu Z, Kaal A, Pedersen SB, Gravholt CH, Andersen JL, Saltin B and Schmitz O (1997) Evidence of an increased number of type IIb muscle fibres in insulin-resistant first-degree relatives of patients with NIDDM. *Diabetes* **46:** 1822–1828.

Potter RF and Groom AC (1983) Capillary diameter and geometry in cardiac and skeletal muscle studied by means of corrosion casts. *Microvasc Res* **25:** 68–84.

Pullen AH (1977) The distribution and relative sizes of fibre types in the extensor digitorum longus and soleus muscles of the adult rat. *J Anat* **123:** 467–486.

Punkt K, Unger A, Welt K, Hilbig H and Schaffranietz (1996) Hypoxia-dependent changes of enzyme activities in different fibre types of rat soleus and extensor digitorum longus muscles. A cytophotometrical study. *Acta Histochem (Jena)* **98:** 255–269 (R1154–R1162).

Ranvier L (1874) De quelques faits relatifs à l'histologie et à la physiologie des muscles stries. *Arch Physiol Norm Path* **6:** 1–15.

Romanul FCA (1965) Capillary supply and metabolism of muscle fibres. *Arch Neurol* **12:** 497–509.

Schaper W, Gorge G, Winkler B and Schaper J (1988) The collateral circulation of the heart. *Prog Cardiovasc Dis* **31:** 57–77.

Schaper W, Sharma HS, Quinkler W, Markert T, Wünsch M and Scharper J (1990) Molecular biologic concepts of coronary anastomoses. *J Am Coll Cardiol* **15:** 513–518.

Schiaffino S, Gorza L, Sartore S, Saggin L, Ausoni S, Vianello M, Gundersen K and Lømo T (1989) Three myosin heavy chain isoforms in type 2 skeletal muscle fibres. *J Musc Res Cell Motil* **10:** 197–205.

Stål P, Eriksson PO and Thornell LE (1996) Differences in capillary supply between human oro-facial, masticatory and limb muscles. *J Musc Res Cell Motil* **17:** 183–197.

Symes JF, Losordo DW, Vale PR, Lathi KG, Esakof DD, Mayskiy M and Isner JM (1999) Gene therapy with vascular endothelial growth factor for inoperable coronary artery disease. *Ann Thorac Surg* **68:** 830–836.

Takeshita M, Ina K, Kitamura H, Shimada T and Nakamura M (1997) Ultrastructural study of capillary and myocytic changes in the masseter and heart of KK-Ay mice. *J Electron Microsc* **46:** 413–423.

Tomori Z, Matis L, Karen P, Kubínová L and Krekule I (2000) STESYS2: Extended STESYS software for MS Windows. *Physiol Res* **49:** 695–701.

Williams DA and Segal SS (1992) Microvascular architecture in rat soleus and extensor digitorum longus muscles. *Microvasc Res* **43:** 192–204.